Supporting information

Origin of Sputter Damage during Transparent Conductive Oxide Deposition for Semitransparent Perovskite Solar Cells

Qing Yang[1,3], Weiyuan Duan[1], Alexander Eberst[1,3], Benjamin Klingebiel[1], Yueming Wang[1,4], Ashish Kulkarni[1,5], Andreas Lambertz[1], Karsten Bittkau[1], Yongqiang Zhang[2], Svetlana Vitusevich[2], Uwe Rau[1,3*], Thomas Kirchartz[1, 4], Kaining Ding[1, 3*]*

[1]IEK-5 Photovoltaics, Forschungszentrum Jülich GmbH, Wilhelm-Johnen Straße, 52425 Jülich, Germany

[2]IBI-3 Institute of Biological Information Processing, Forschungszentrum Jülich GmbH, Wilhelm-Johnen Straße, 52425 Jülich, Germany

[3]Faculty of Electrical Engineering and Information Technology, RWTH Aachen University, 7 Mies-van-der-Rohe-Straße 15, 52074 Aachen, Germany

[4]Faculty of Engineering and CENIDE, University of Duisburg-Essen, Carl-Benz-Str. 199, 47057 Duisburg, Germany

[5]Institute of Inorganic Chemistry, Greinstr. 6, University of Cologne, 50939 Cologne

*Correspondence to: w.duan@fz-juelich.de (W.D.), u.rau@fz-juelich.de (U.R.), k.ding@fz-juelich.de (K.D.)

Materials and methods

Materials

The materials were purchased from different suppliers. Cesium iodide (CsI, 99.9%), N,N-dimethylformamide (DMF, 99.8%), dimethyl sulfoxide (DMSO, 99.5%), anisole (99.7%), toluene (99.8%) and ethyl acetate (99.8%) were purchased from Sigma Aldrich. Lead iodide (PbI_2, 99.99%), Me-4PACz (99.9%) and 2PACz (98%) were purchased from TCI. Lead (II) bromide ($PbBr_2$, 98+%) was purchased from Acros Organics. Formamidinium iodide (FAI, 99.99%) and methylammonium iodide (MAI, 99.99%) were purchased from Greatcell. Methylammonium bromide (MABr, 99.99%) was purchased from Dyesol. Fullerene (C_{60}, 99.5%) was purchased from

Ossila. Quartz glass (QG) with a thickness of 1 mm was purchased from A.L.L Lasertechnik GmbH. Magnesium fluoride-coated glass (MgF_2) was purchased from Korth Kristalle GmbH, which is a MgF_2-VUV-window with a thickness of 1 ± 0.1 mm.

Layer stacks fabrication

Three types of layer stacks were prepared, with and without ITO: 1) glass/ITO/2PACz/perovskite stacks, 2) glass/ITO/2PACz/perovskite/C_{60} stacks, and 3) glass/ITO/2PACz/perovskite/C_{60}/SnOx stacks. The pre-patterned ITO substrates (2.0 × 2.0 cm^2) were bought from Yingkou Youxuan Trade Co, Ltd and ultrasonically cleaned with soap (Hellmanex III), deionized water, acetone, and IPA in succession for 10 min. The as-cleaned glass/ITO substrates were treated with oxygen plasma (Diener Zepto, 50 W) for 12 min and immediately transferred to a N2-filled glovebox. 80 µL of 2PACz (0.3 mg/ml in dry alcohol) solution was spin-coated onto the ITO substrates at 3000 rpm for 30 s (with a ramping rate of 1000 rpm/s), followed by thermal annealing at 100 ˚C for 10 min and afterwards cooled down to room temperature. The perovskite precursors were prepared using a typical triple-cation process. PbI_2 and $PbBr_2$ were dissolved in a solution of DMF: DMSO = 4:1 in volume and stirred at 60 ˚C overnight, then the 1.5 M nominal stock solutions were added to FAI and MABr with 9% PbX_2 excess, respectively (X= I or Br), and stirred for 10 min at 60 ˚C. $FAPbI_3$ and $MAPbBr_3$ were mixed in a volume ratio of 5:1 to obtain $FA_XMA_{1-X}Pb(I_XBr_{1-X})_3$ and stirred for 10 min at 60 ˚C. Finally, 5 vol% of 1.5 M nominal CsI in DMSO was added to the obtained "triple cation" perovskite and stirred at 60 ˚C for 10 min. 110 µl of perovskite (1.63 eV) was spread on the glass/ITO/2PACz layer stacks and spin-coated at 5500 rpm for 35 s (with a ramping rate of 800 rpm/s) using one-step spin-coating method. 10 s before the end of the program, 300 µL of anisole as the anti-solvent was drop-cast onto the spinning substrates, the films were immediately annealed on a hot plate at 100 ˚C for 30 min. 20 nm C_{60} was thermally evaporated in a separate vacuum chamber (< 5×10^{-6} Pa). Subsequently, a 15 nm SnO_X layer was deposited at 80 ˚C using ALD (TFS200, Beneq). Tetrakis (dimethylamino)tin(IV) (TDMASn) and deionized water as tin and oxygen precursors, respectively, were heated to 55 °C and maintained at room

temperature. Nitrogen (N_2) was used as the carrier gas at a flow rate of 500 sccm, and the inner chamber was continuously purged. One cycle of the ALD process consisted of the following sequence: TDMASn pulse (1 s)/ N_2 purge (30 s)/ water (1 s)/ N_2 purge (30 s). The thickness and homogeneity of the SnO_X grown on 4-inch mirror-polished c-Si wafers were characterized by ellipsometry with a growth rate of 1.5 Å per cycle and a well-controlled thickness variation below 1 nm. The 110 nm ITO electrode was then sputtered on top of the SnO_X with and without optical filter shading via radio frequency (RF) magnetron sputtering at a background pressure below 2◊10^{-5} Pa and a temperature of 40 ˚C. The ceramic target consisted of 95 wt. % In_2O_3 and 5 wt. % SnO_2 with a diameter of 96 mm. The sputtering power used in this study was 50 W, with a power density of 0.69 W/cm^2. The flow rate ratio of Ar/O_2 and the working pressure were set to 14:1 and 0.5 Pa, respectively. The sputtering process required 35 min at a deposition rate of 2.9 nm/min.

Single-junction opaque perovskite solar cells

The fabrication of single-junction opaque perovskite solar cells was similar to that described for layer stacks, with a few differences. Following C_{60} deposition, half of the semi-devices were shielded with optical filters and treated with the plasma radiation generated by ITO sputtering, while the remaining semi-devices covered with an opaque mask were kept in the sputtering chamber at the same time. Finally, 8/80 nm BCP/Ag was thermally evaporated on all semi-devices.

Semi-transparent perovskite solar cells

The as-cleaned glass/ITO substrates were treated with oxygen plasma for 12 min and transferred to a N_2-filled glovebox for the following process. 80 µL of Me-4PACz (0.3 mg/ml in dry alcohol) solution was spin-coated onto the substrates at 3000 rpm for 30 s (with a ramping rate of 1000 rpm/s), followed by thermally annealing at 100 ˚C for 10 min and afterwards cooled down to room temperature. The perovskite precursors were prepared with a higher band gap (1.68 eV) for better performance by mixing PbI_2 (0.67 M), FAI (0.73 M), $PbBr_2$ (0.33 M), MAI (0.22 M) and CsI (0.05 M) in DMF/DMSO, stirred at 60 ˚C for 1 h and filtered with a 0.45 µm PTFE filter. 110 µL of

perovskite was spread on top of the Me-4PACz layer by a two-consecutive step spinning program at 2000 rpm for 15 s (4s acceleration) and 6000 rpm for 60 s (5s acceleration). 30 s before the end of the program, 300 µL of anisole as the anti-solvent was drop-cast onto the spinning substrates, and the films were immediately annealed on a hot plate at 100 ˚C for 20 min. Consequently, 20 nm/15 nm/110 nm C_{60}/(SnO_X/)ITO stacks were deposited on the perovskite. Finally, 80 nm Ag was thermally evaporated using a well-designed shadow mask with an aperture area of 0.16 cm^2.

Characterization

Steady-state photoluminescence (ssPL) was performed to investigate the non-radiative recombination. This was accomplished using a laser with a wavelength of 532 nm and spot size of 0.10 cm^2. The laser intensity was set to replicate the solar intensity equivalent to 1 sun. X-ray diffraction (XRD) was performed to investigate the crystal structural changes using a RIGAKU SmartLab with a Cu Kα radiation source. The X-ray generator was set to 40 kV and 40 mA, and 2θ scans between 5° and 60° were collected with a step size of 0.02°.

X-ray photoelectron spectroscopy (XPS) was performed to investigate the local chemical bonding on surface using a MULTIPROBE MXPS system from Scienta Omicron with an ARGUS hemispherical electron spectrometer, which is part of the JOSEPH cluster system in the research center Jülich. The samples were transferred from the glovebox to the UHV cluster under inert gas. The base pressure in the XPS system was $1 \cdot 10^{-10}$ mbar.

The X-ray excitation source was an XM 1000 Al Kα X-ray excitation source operated at 300 W. The resulting spectra were collected in constant Analyzer-Energy (CAE) mode with path energies of 100 eV for the survey spectrum and 20 eV for the high-resolution spectra, respectively.

The *JV* characteristics were measured using a calibrated AM1.5 spectrum of a class ABB solar simulator (Lot Oriel LCS-100) directly integrated into the glovebox, which was also used for maximum power point (MPP) tracking. A monocrystalline silicon reference cell (Oriel 91150V) provided a power density of 100 mW/cm^2, which was certified by Newport Corporation's PV Lab (North Logan, UT), an ISO/IEC 17025 accredited photovoltaic calibration and test laboratory. The measurements were performed in accordance with the ASTM E948 and E1021 standard methods

developed and used by the United States National Renewable Energy Laboratory (NREL). An illumination mask with an aperture area of 0.81 cm^2 was used for *JV* measurements of tandem cells.

The external quantum efficiency (EQE) setup consisted of a xenon light source (Osram XPO150W) and Bentham monochromator (TMC300) with a spectral range of 300-1150 nm. A calibrated silicon photodiode (Gigahertz-Optik SSO-PD100-04) was used as a reference for simulated light calibration. The device was placed behind a quartz glass window in a sealed nitrogen-filled measurement box during the measurement to prevent performance degradation. Thus, a lower integrated current density was obtained compared with the short-circuit current density extracted from the *JV* curve.

SRIM simulations

To simulate the penetration depth of negative ions with an initial kinetic energy of 85 eV, 2000 phonons were computed using the Stopping and Range of Ions in Matter (SRIM) program. The density setup of perovskite, C_{60} and SnO_X were 4.59 g/cm^3, 1.65 g/cm^3, 6.85 g/cm^3, respectively. The damage model and basic plot were Ion Distribution and Quick Calculation of Damage and Ion Distribution with Recoils projected on Y-plane, respectively.

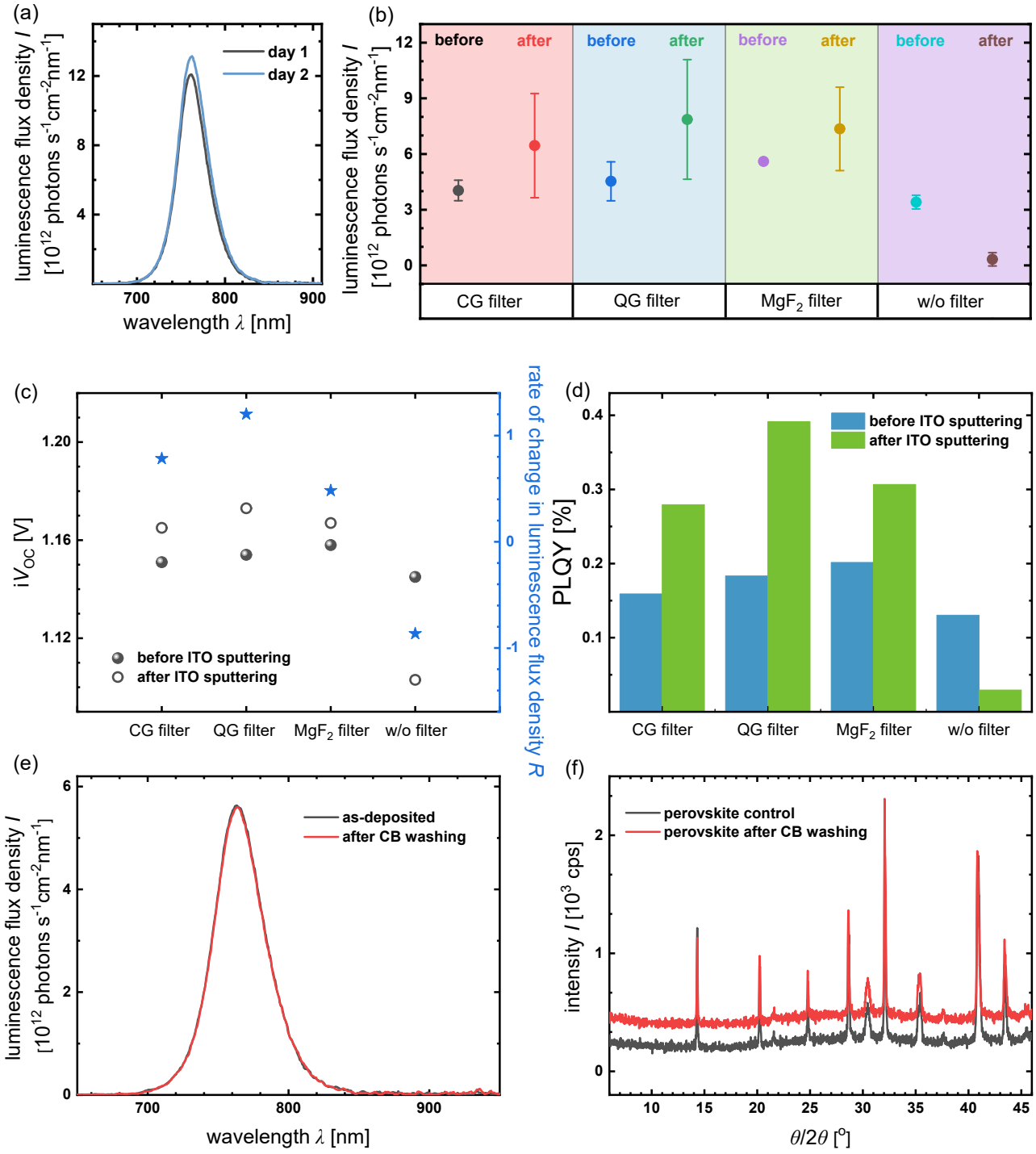

Fig S1. a) Short-term stability of the samples for PL measurements. b) Statistical data of PL intensity, c) rate of change in PL intensity and its implied open-circuit voltage (iV_{OC}), and d) PLQY of stacks shielded by CG filter, QG filter, MgF_2 filter, w/o filter before and after ITO sputtering.

e) PL spectra and f) XRD patterns of the perovskite before and after CB washing.

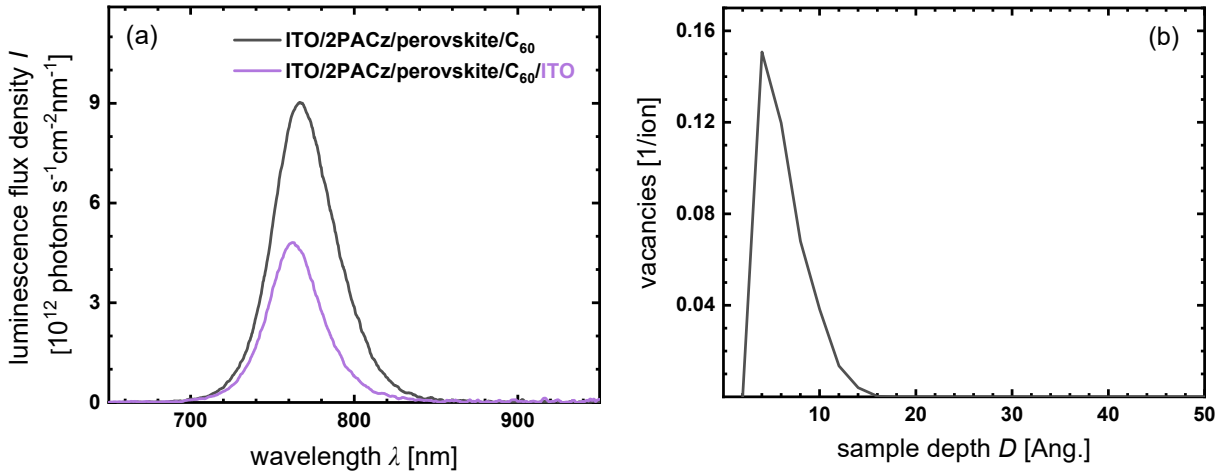

Fig. S2. a) Spectra of the stacks with 35 nm-thick C_{60} before and after ITO sputtering. b) Distribution of target vacancies in the C_{60} layer after the lattice atoms were knocked out of the original site by oxygen ions.

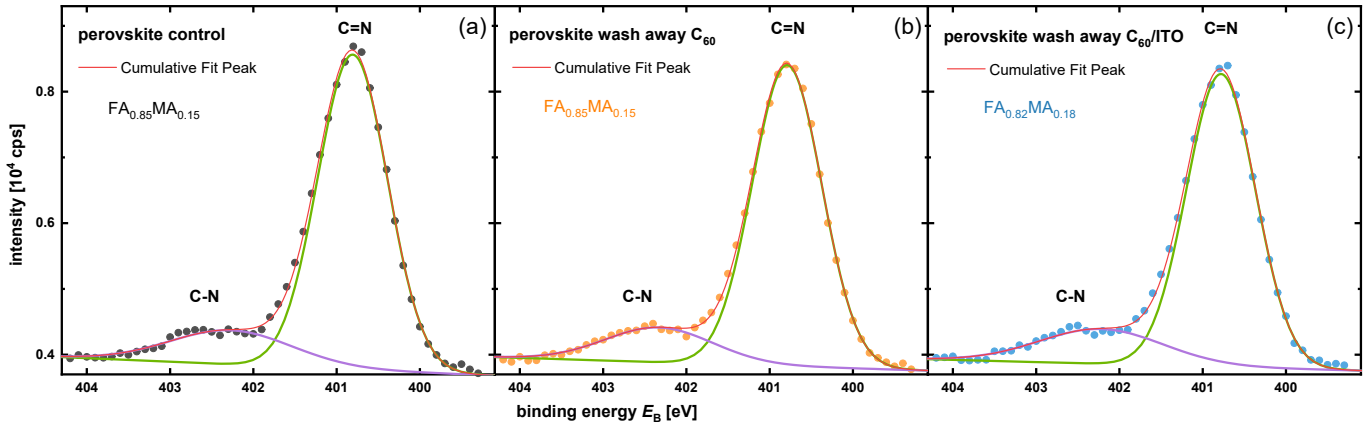

Fig. S3. N 1s peak fitting of a) the controlled perovskite film, b) perovskite films with C_{60}, and c) C_{60}/ITO washed away.

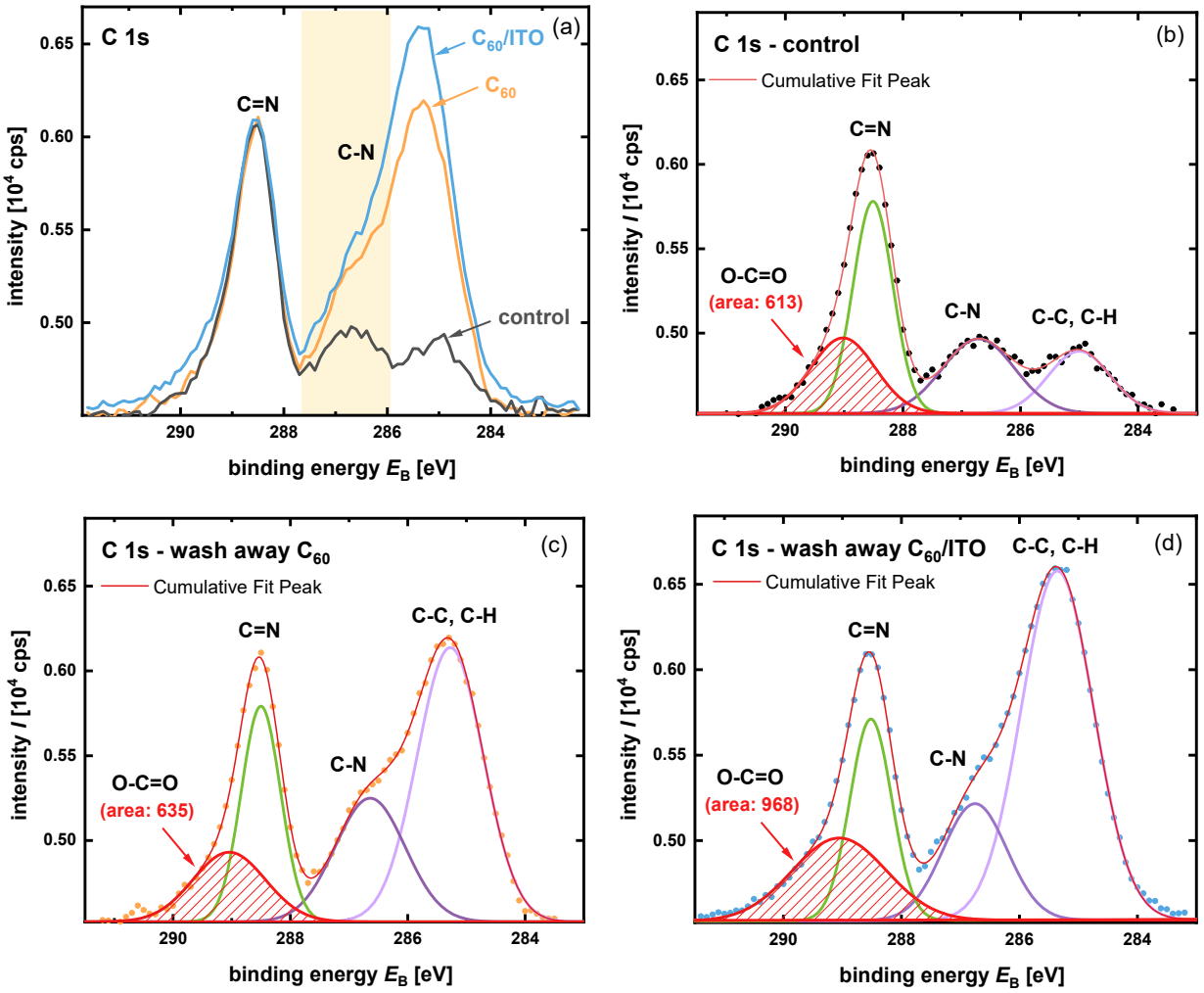

Fig. S4. XPS spectra of a) C 1s peaks of three samples. The relevant C 1s peak fitting of b) the controlled perovskite film, c) perovskite films with C_{60}, and d) C_{60}/ITO washed away.

Table 1. The full width at half maximum (FWHM) values before and after ITO sputtering in the four scenarios

	FWHM [nm]			
	CG filter	QG filter	MgF_2 filter	Without filter
Before ITO	41.8	41.8	41.7	41.3
After ITO	42.3	41.4	41.6	40.7

Table 2. XPS data for the deconvoluted peaks of C=N bonds in the C 1s core level spectra of the three samples.

Samples	Ration of O=C-O/C=N	FWHM [eV]	Max height [cps]	E_B [eV]
Control	0.36	0.80 (±0.07)	1257	288.5 (±0.01)
Wash away C_{60}	0.37	0.79 (±0.04)	1271	288.5 (±0.01)
Wash away C_{60}/ITO	0.48	0.83 (±0.04)	1180	288.5 (±0.01)

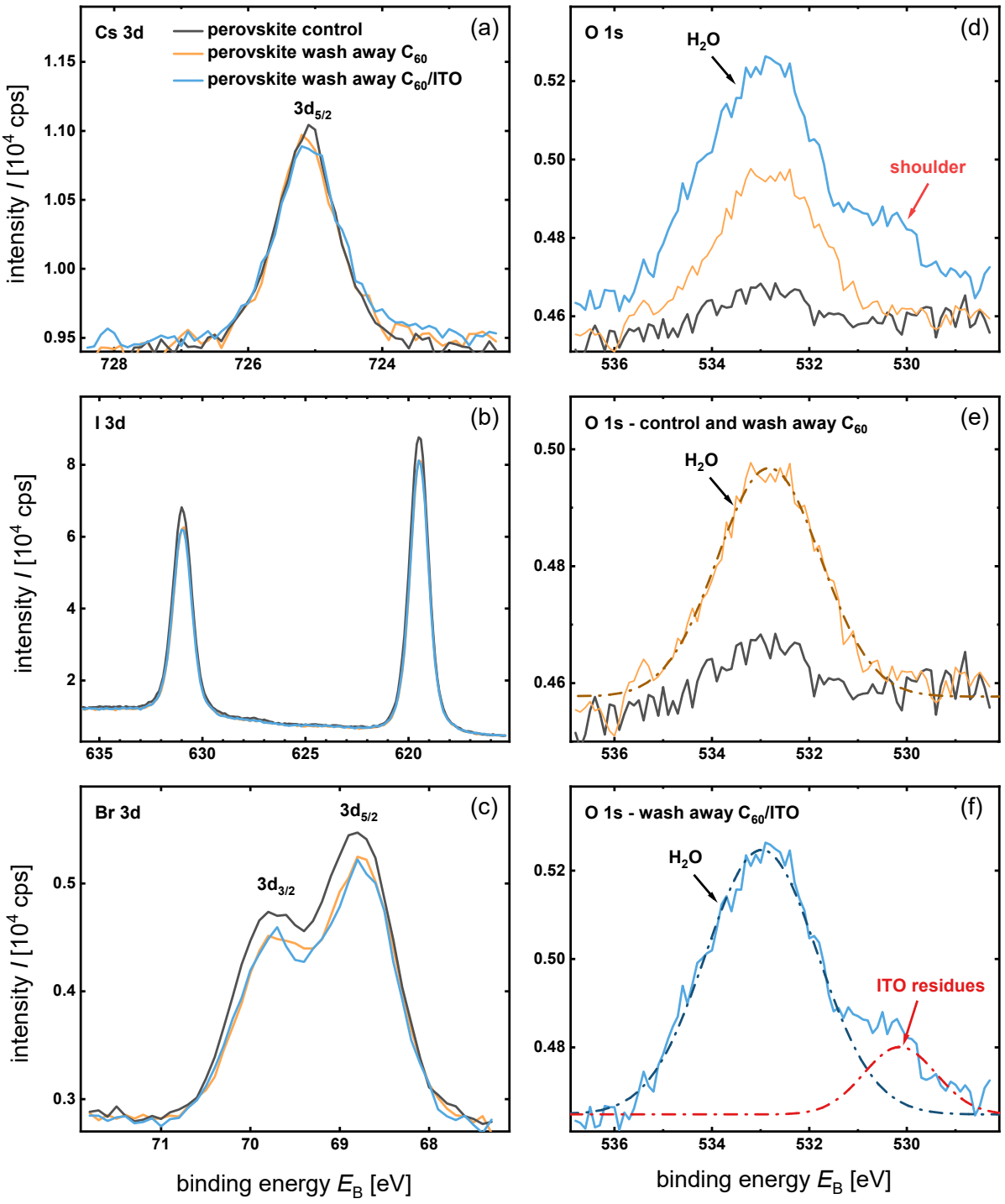

Fig. S5. XPS spectra of a) Cs 3d, b) I 3d, c) Br 3d and d-f) O1s peaks of three samples.

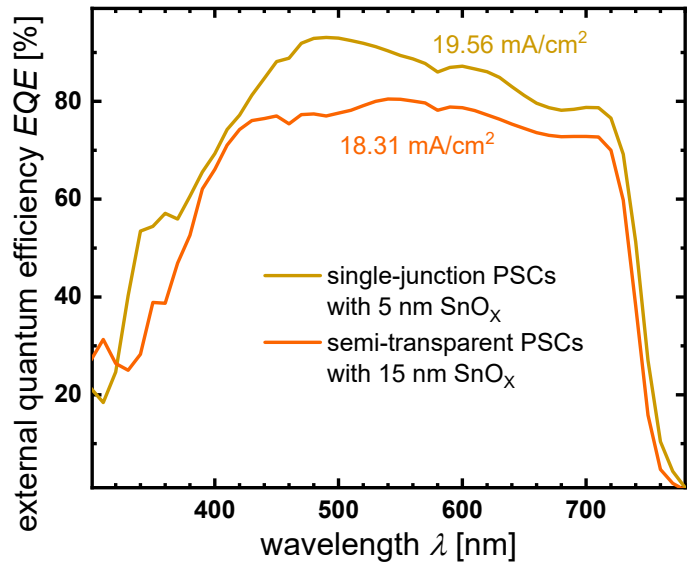

Fig. S6. EQE of single-junction and semi-transparent perovskite solar cells.

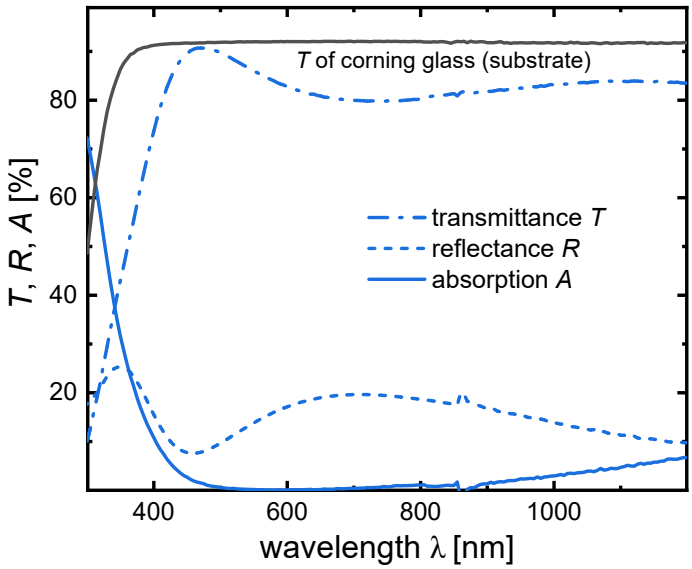

Fig. S7. Transmittance, reflectance, and absorption of bare ITO film sputtered on a glass substrate.

Table 3. Electrical parameters of bare ITO film sputtered on a glass substrate.

Thickness [nm]	Sheet resistance [Ω/sq]	Mobility [cm^2/Vs]	Carrier concentration [10^{20} cm^{-3}]	Resistivity [10^{-4} Ω.cm]
110	40	29.8	5.0	4.2

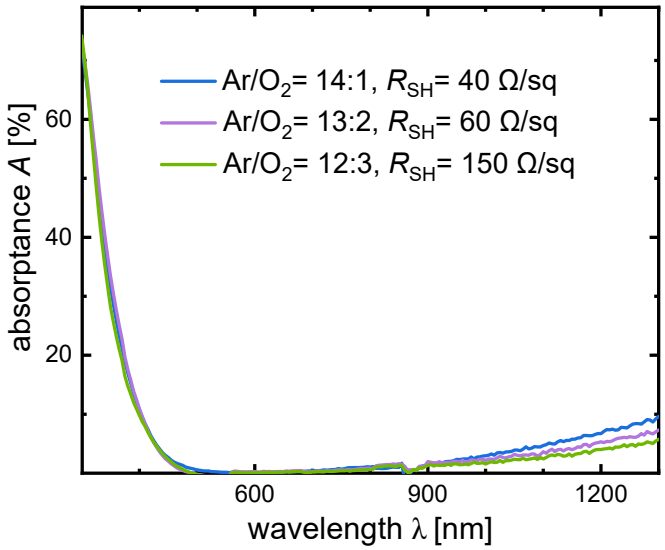

Fig. S8. Absorption of bare ITO films as a function of Ar/O_2 flow rate ratio. Note that an additional oxygen flow was introduced to tune the optical and electrical properties of the ITO films. The sheet resistance increased as the oxygen content increased, owing to a reduction in oxygen vacancies, resulting in additional electrical losses. However, the absorption of ITO decreases in the long-wavelength range owing to a reduction in the absorption of the free carriers. The increase in the oxygen content did not increase the sputtering damage because the ion bombardment of the samples was primarily affected by the sputtering power and working pressure at a low deposition temperature.

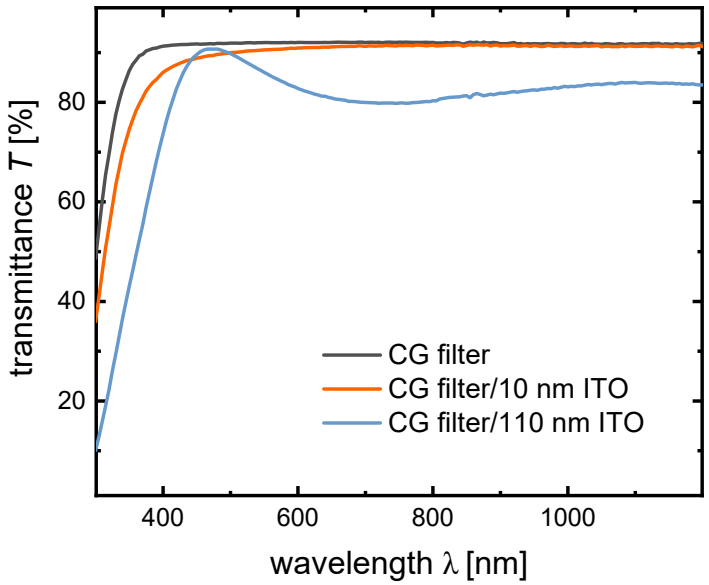

Fig. S9. Transmittance of the 10 nm and 110 nm ITO films on the CG filter.

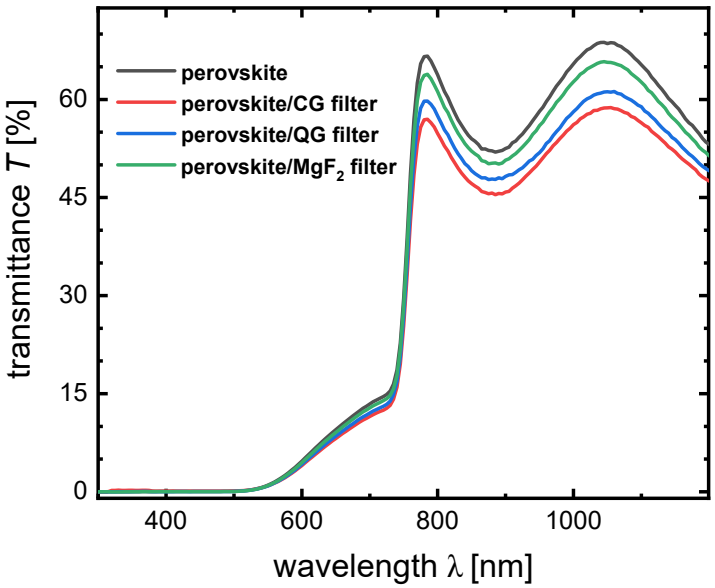

Fig. S10. Transmittance of the perovskite film before and after using CG, QG, and MgF_2 filters.

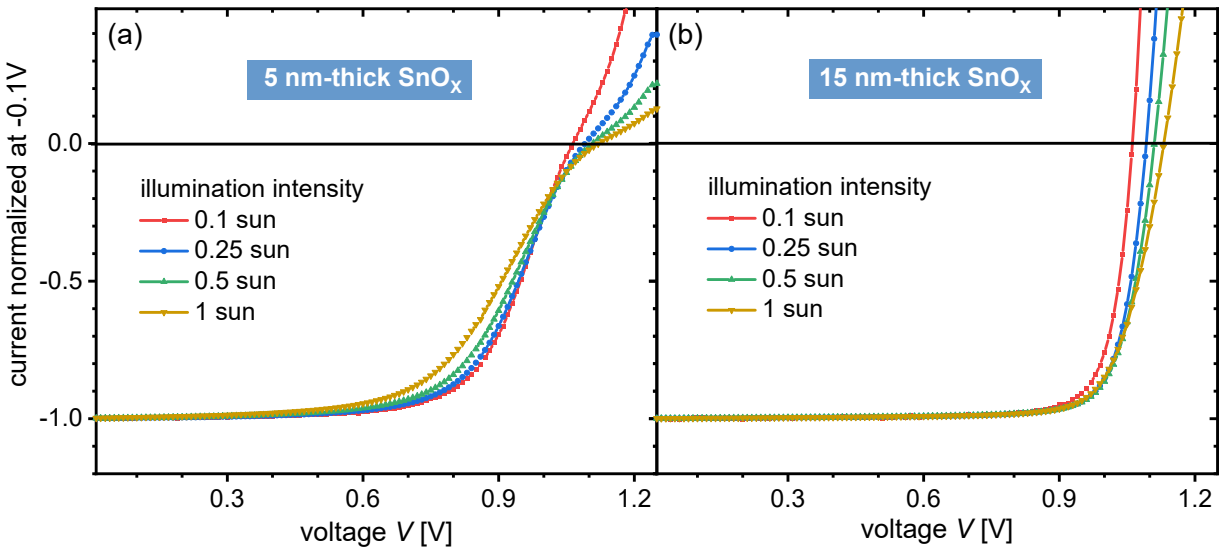

Fig. S11. *JV* curves at several illumination intensities, from 0.1 to 1 sun, normalized at -0.1 V, for a) semi-transparent perovskite solar cells with a 5 nm-thick SnO_X film and b) with a 15 nm-thick SnO_X film. We adapted the method based on the analyses of current–voltage data as a function of illumination intensity to reveal the origin of the S-shape.[1]

Reference

1. W. Tress and O. Inganäs, *Sol. Energy Mater. Sol. Cells*, 2013, **117**, 599-603.